Electronic Supplementary Information for

Composite interface of g-C_3N_4 fragment loaded on Cu substrate for CO_2 reduction

Qiang Gong, Jianling Xiong, Tanyu Zhou, Wenkai Bao, Xiuyun Zhang, Guiwu Liu*, Guanjun Qiao and Ziwei Xu*

[a.]School of Materials Science and Engineering, Jiangsu University, Zhenjiang 212013, China.
[b.]College of Physics Science and Technology, Yangzhou University, Yangzhou 225002, China.
*E-mail address: ziweixu2014@ujs.edu.cn (Z. Xu); gwliu76@ujs.edu.cn（G. Liu）

Setup of DFT calculations

The three C_3N_4/Cu systems have been modeled by two layers of Cu atoms and one layer C_3N_4 fragments. During structure optimizations, the adsorbates, g-C_3N_4 fragment, and top layer of the Cu atoms are allowed to move freely. The lattice parameters for C_3N_4/Cu(111) and C_3N_4/Cu(111)-b are set as a=b=15.34 Å, c=30 Å, α =β =90°, γ=120.00°. For C_3N_4/Cu(110) and C_3N_4/Cu(110)-b, they are a=21.69 Å, b=15.34 Å, c=30 Å, α =β =γ= 90°; For C_3N_4/Cu(100) and C_3N_4/Cu(100)-b, they are a=b=15.34 Å, c=30 Å, α=β=γ=90°, respectively.

Definitions of adsorption energy (E_{ad}), free energy change (ΔG) and binding energy ($E_{binding}$)

The adsorption energies (E_{ad}) are calculated by the following equations.

$E_{ad} = E_{tot} - E_{substrate} - E_{adsorbate}$

Where E_{tot}, $E_{substrate}$and $E_{adsorbate}$ are the energies of substrate with adsorbates, the substrate catalysts, and the isolated adsorbates, respectively. All energies above are obtained under the same parameter settings.

For each reaction step of CO_2RR, the free energy changes (ΔG) are using the computational hydrogen electrode (CHE) model, which are expressed by the following equations

$$\Delta G = \Delta E + \Delta E_{ZPE} - T\Delta S + \Delta G_{PH}$$

Where ΔE is the changes in the reaction energy. ΔE_{ZPE} and ΔS are the differences in zero point energy and entropy, respectively, between the two states. T is the temperature (298.15 K). ΔG_{PH} is expressed as $\Delta G_{PH} = K_B T \ln 10 \times pH$, and in this work, the pH is set as 0.

To evaluate the stability of the different C_3N_4/Cu configurations, the binding energy of the composite structure of C_3N_4/Cu is expressed by the following equation

$$E_{binding} = E_{C_3N_4/Cu} - E_{Cu} - E_{C_3N_4}$$

Where $E_{C_3N_4/Cu}$, E_{Cu} and $E_{C_3N_4}$ are the energies of the C_3N_4/Cu, the Cu substrate, and the fragment of g-C_3N_4.

Definitions of limiting potential (U_L) and overpotential (η)

The limiting potential (U_L) is calculated by the following equations:

$$U_L = -\frac{\Delta G_{max}}{e}$$

The U_L is the minimum negative potential that makes each basic step exothermic. Where ΔG_{max} is the maximum free energy rise for the entire CO_2RR path. The overpotential (η) is evaluated as the difference between the equilibrium potential and the limiting potential. Therefore, the overpotential is defined as

$$\eta = U_0 - U_L$$

where U_0 and U_L is the equilibrium potential and limiting potential, respectively.

CO_2RR pathways

For CO_2RR, the main consideration is the hydrogenation of *CO to form *CHO followed by the hydrogenation to form CH_3OH or CH_4. The main possible pathways are as follows

*CHO/*COH→*CHOH→*CH+H_2O→*CH_2→*CH_3→*CH_4 (1)

*CHO/*COH→*CHOH→*CH_2OH→*CH_2+H_2O→*CH_3→CH_4 (2)

CHO→OCH_2→*OCH_3→*OCH_4→*OH+CH_4→H_2O (3)

*COH→*C+H_2O→*CH→*CH_2→*CH_3→CH_4 (4)

*CHO/*COH→*CHOH→*CH_2OH→CH_3OH (5)

In eqn (3), *OCH_3 is not generated stably in C_3N_4/Cu composite system. Therefore, eqn (3) is not considered. However, the formation of *COH intermediates always involves a high energy barrier compared with *CHO. Therefore the main consideration of CH_4 and CH_3OH production in this work is the path of *CHO in eqn(1) , eqn(2) and eqn(5).

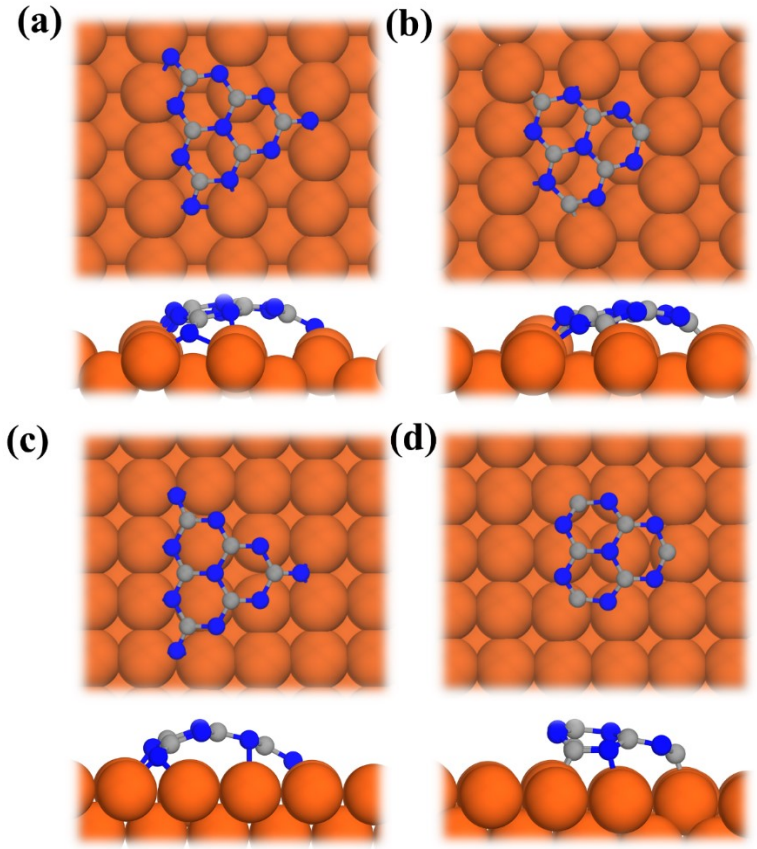

Figure S1. The top and side views of (a) C_3N_4/Cu(110) (b) C_3N_4/Cu(110)-b (c) C_3N_4/Cu(100) and (d) C_3N_4/Cu(100)-b.

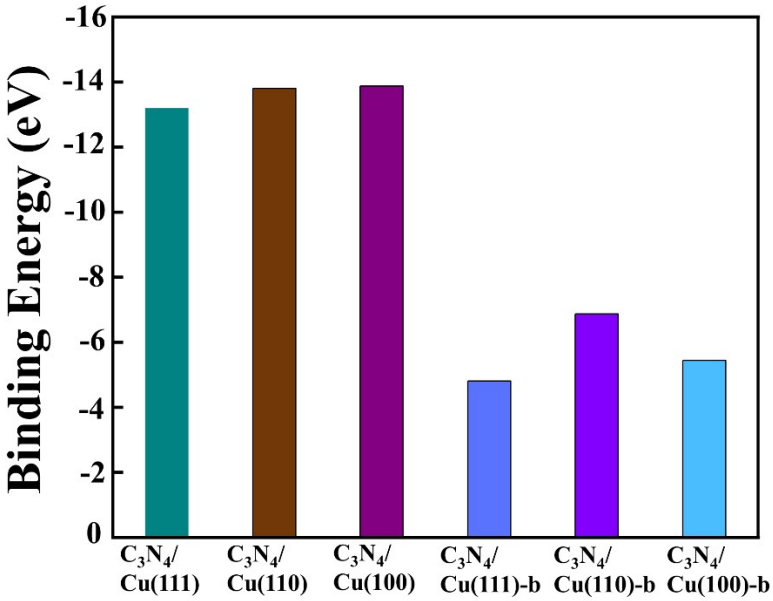

Figure S2. Binding energies of structures for two different g-C_3N_4 fragments loaded on different Cu facets.

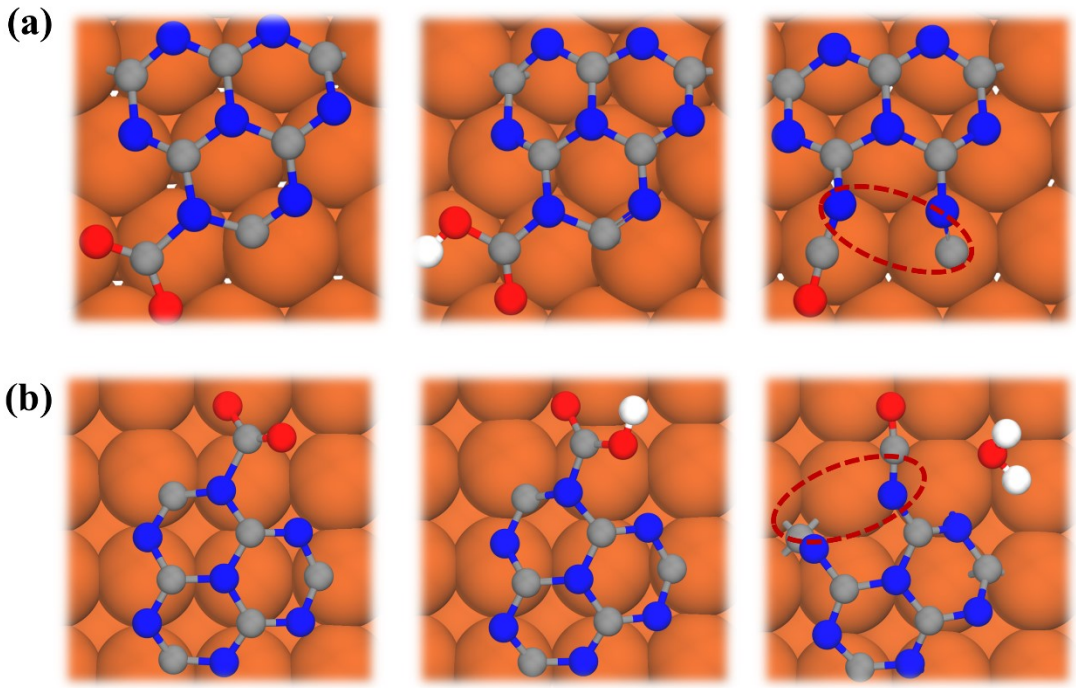

Figure S3. The structures transformations of CO_2 reduced to CO pathway on (a) C_3N_4/Cu(111)-b and (b) C_3N_4/Cu(100)-b, the red lines highlight the destructed g-C_3N_4 fragments.

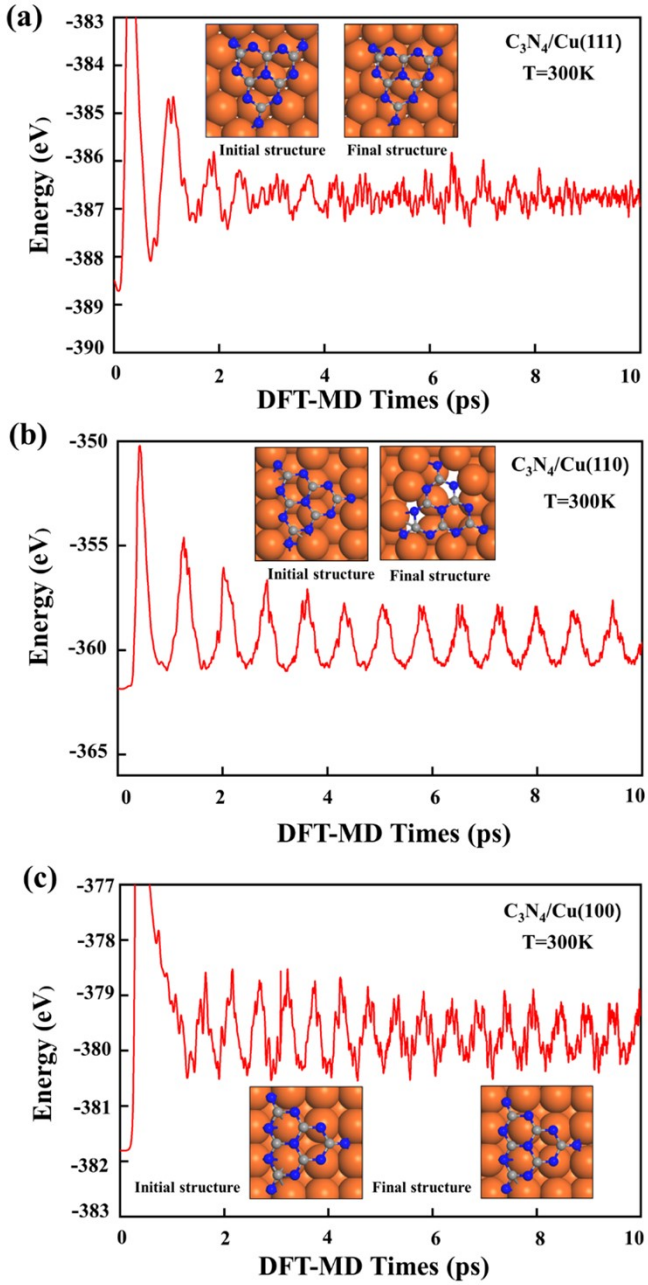

Figure S4. The total energy as a function of MD time. (a) C_3N_4/Cu(111), (b) C_3N_4/Cu(110), (c) C_3N_4/Cu(100). The inset shows the initial and final structures.

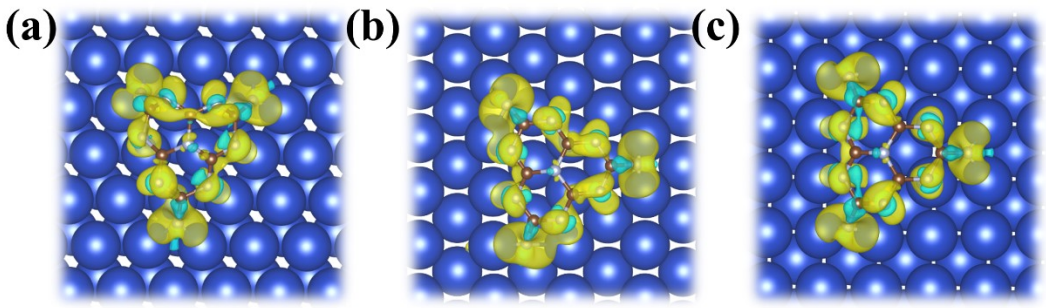

Figure S5. The charge difference densities (CDD) of (a) C_3N_4/Cu(111), (b) C_3N_4/Cu(110) and (c)

C_3N_4/Cu(100). The isosurface value is 0.001e/Å^3. Yellow and cyan represent charge accumulation and depletion, respectively. The grey, white, and blue balls represent carbon, nitrogen, copper atoms, respectively.

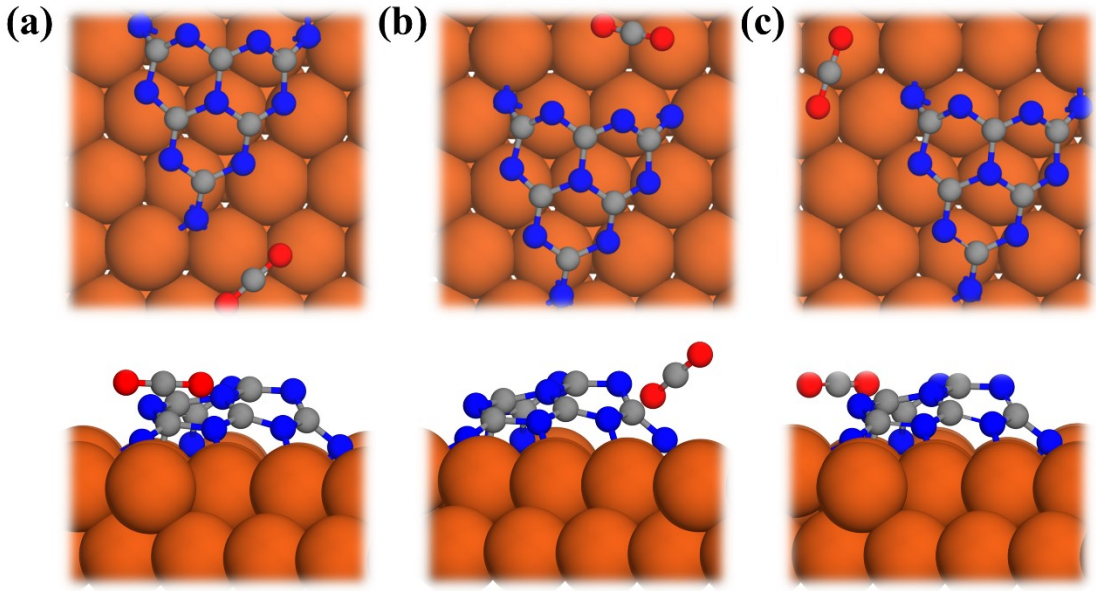

Figure S6. The top and side views of optimized structures of CO_2 adsorptions on (a) N1, (b) N2 and (c) N3 sites with O-N position on C_3N_4/Cu(111).

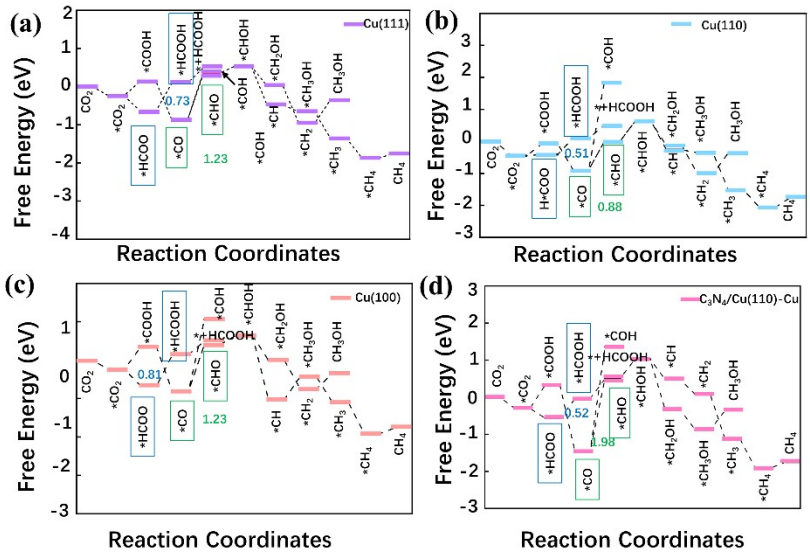

Figure S7. The calculated free energy pathways for CO_2RR on the (a) Cu (111), (b) Cu(110), (c) Cu(100) and (d) Cu sites near C_3N_4/Cu(110) interface. The ΔG_{max} and PDS for CH_4 and CH_3OH are same, which is highlighted in green. The ΔG_{max} and PDS for HCOOH is highlighted in blue.

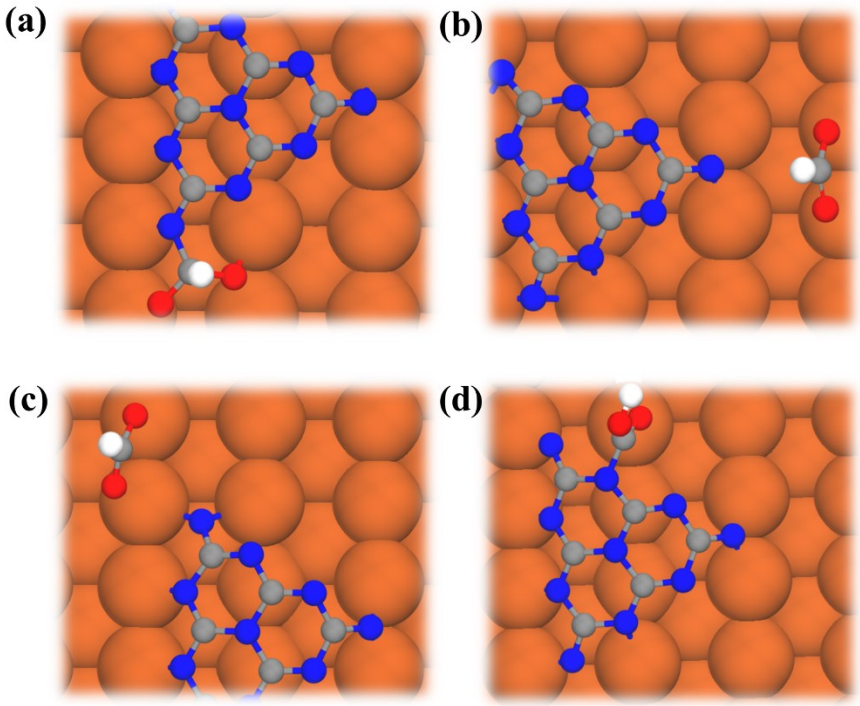

Figure S8. The *HCOO on (a) C_3N_4/Cu(110)-N1, not stably formed on (b) C_3N_4/Cu(110)-N2, (c) C_3N_4/Cu(110)-N3 and (d) C_3N_4/Cu(110)-E4.

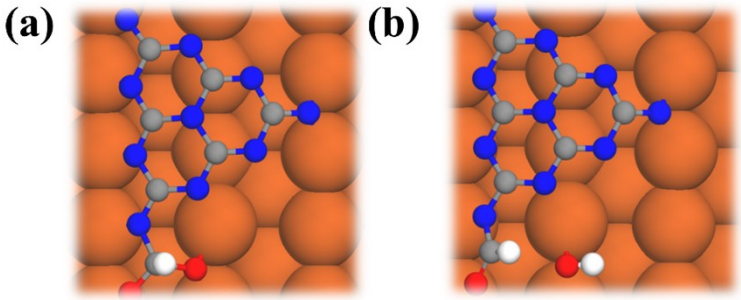

Figure S9. (a) *HCOO and (b) *CHO+*OH on C_3N_4/Cu(110)-N1.

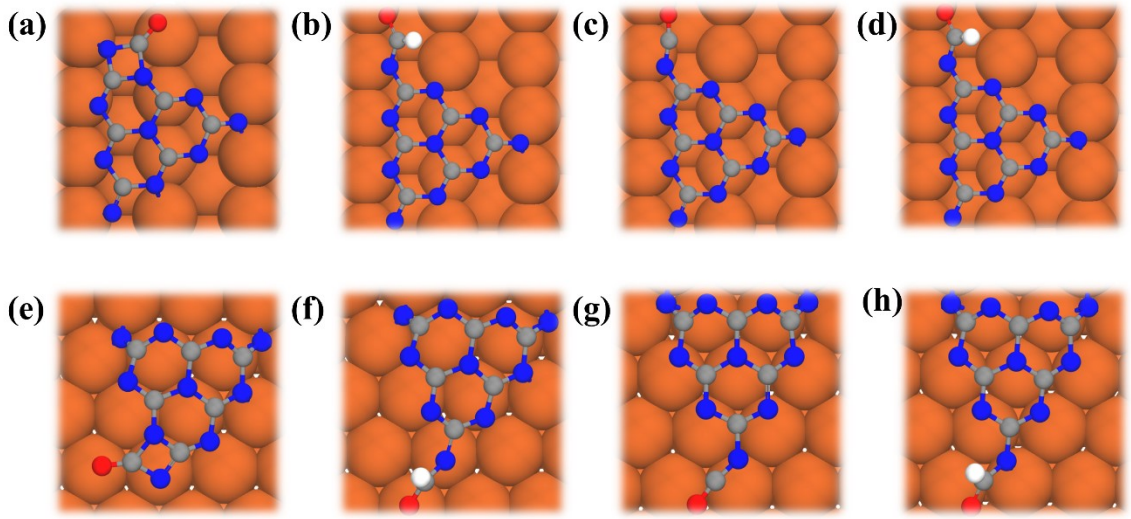

Figure S10. (a-d) The *CO and *CHO formed on C_3N_4/Cu(110)-E4 and C_3N_4/Cu(110)-N3, respectively, (e-h) The *CO and *CHO formed on C_3N_4/Cu(111)-E6 and C_3N_4/Cu(111)-N1, respectively.

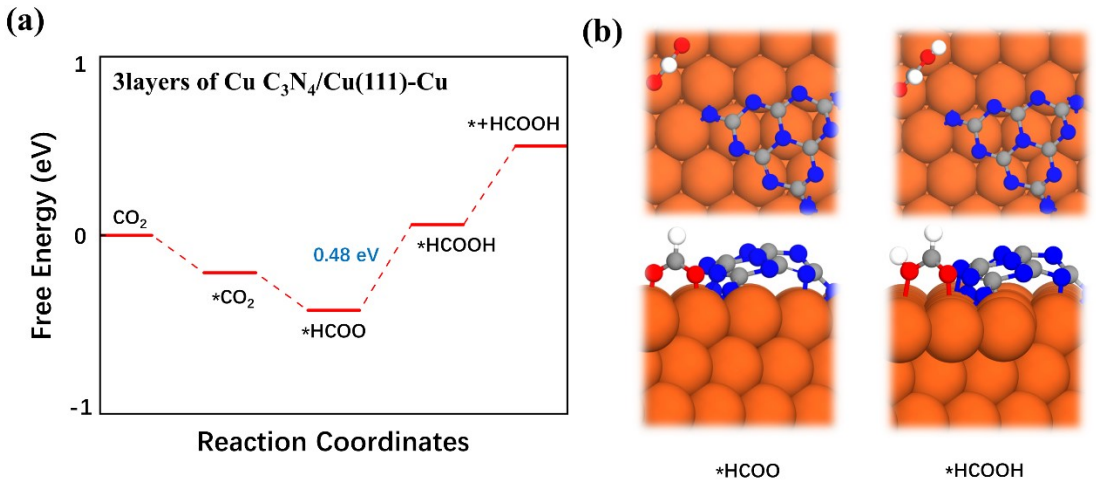

Figure S11 (a) The free energy pathways of 3 layers of Cu for C_3N_4/Cu(111). The ΔG_{max} is highlighted in blue. (b) The top and side views of *HCOO and *HCOOH on C_3N_4/Cu(111)

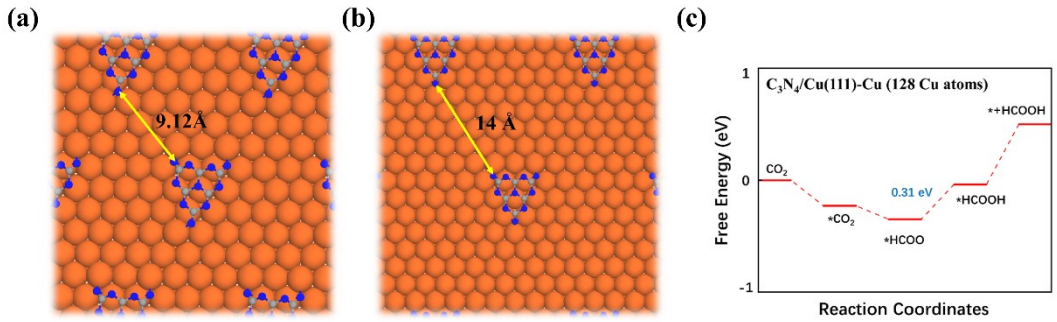

Figure S12 The C_3N_4/Cu(111) structures with different C_3N_4 concentrations. (a) original concentration, (b) lower concentrations (c) The free energy pathways of HCOOH production on the C_3N_4/Cu(111)-Cu with lower C_3N_4 concentration. The ΔG_{max} is highlighted in blue.

Table S1 The adsorption energies of CO_2 adsorbed on the different Cu sites near the C_3N_4/Cu interfaces.

Sites	E_{tot}(eV)	$E_{substrate}$ (eV)	E_{CO_2}(eV)	E_{ad} (eV)
C_3N_4/Cu(111)-Cu-top--	-416.3	-393.09	-22.98	**-0.23**
C_3N_4/Cu(111)-Cu-hcp	-416.31	-393.09	-22.98	-0.24
C_3N_4/Cu(111)-Cu-fcc	-416.28	-393.09	-22.98	-0.21
C_3N_4/Cu(111)-Cu-bridge	-416.3	-393.09	-22.98	-0.23
C_3N_4/Cu(110)-Cu-hollow	-383.64	-360.36	-22.98	**-0.3**
C_3N_4/Cu(110)-Cu-bridge-	-383.56	-360.36	-22.98	-0.22
C_3N_4/Cu(110)-Cu-top	-383.56	-360.36	-22.98	-0.22
C_3N_4/Cu(100)-Cu-hollow	-404.94	-381.7	-22.98	**-0.26**
C_3N_4/Cu(100)-Cu-top	-404.9	-381.7	-22.98	-0.22
C_3N_4/Cu(100)-Cu-bridge	-404.94	-381.7	-22.98	-0.26

Table S2 The adsorption energies of CO_2 adsorbed on nitrogen sites of C_3N_4/Cu(111) interfaces with C-N and O-N configurations.

Sites	E_{tot}(eV)	$E_{substrate}$ (eV)	E_{CO_2}(eV)	E_{ads} (eV)
C_3N_4/Cu(111)-N1-C-N-	-416.84	-393.09	-22.98	-0.77
C_3N_4/Cu(111)-N2-C-N	-417.03	-393.09	-22.98	-0.96
C_3N_4/Cu(111)-N3-C-N	-416.55	-393.09	-22.98	-0.48
C_3N_4/Cu(111)-N1-O-N	-416.31	-393.09	-22.98	-0.24
C_3N_4/Cu(111)-N2-O-N	-416.29	-393.09	-22.98	-0.22
C_3N_4/Cu(111)-N3-O-N	-416.3	-393.09	-22.98	-0.23

Table S3 The binding energies between C_3N_4 and 2-layers Cu(111) and 3-layers Cu(111***).***

Structures	E_{total}(eV)	E_{Cu}(eV)	E_{C3N4}(eV)	$E_{binding}$(eV)
C_3N_4/Cu(111) (2layers Cu)	-393.06	-256.93	-122.94	-13.19
C_3N_4/Cu(111) (3layers Cu)	-545.81	-409.18	-122.94	-13.69